Rationally Designed Donor–Acceptor Random Copolymers with Optimized Complementary Light Absorption for Highly Efficient All-Polymer Solar Cells

Sang Woo Kim, Joonhyeong Choi, Thi Thu Trang Bui, Changyeon Lee, Changsoon Cho, Kwangmin Na, Jihye Jung, Chang Eun Song, Biwu Ma, Jung-Yong Lee, Won Suk Shin,* and Bumjoon J. Kim*

Most of the high-performance all-polymer solar cells (all-PSCs) reported to date are based on polymer donor and polymer acceptor pairs with largely overlapped light absorption properties, which seriously limits the efficiency of all-PSCs. This study reports the development of a series of random copolymer donors possessing complementary light absorption with the naphthalenediimide-based polymer acceptor P(NDI2HD-T2) for highly efficient all-PSCs. By controlling the molar ratio of the electron-rich benzodithiophene (BDTT) and electron-deficient fluorinated-thienothiophene (TT-F) units, a series of polymer donors with BDTT:TT-F ratios of 1:1 (P1), 3:1 (P2), 5:1 (P3), and 7:1 (P4) are prepared. The synthetic control of polymer composition allows for precise tuning of the light absorption properties of these new polymer donors, enabling optimization of light absorption properties to complement those of the P(NDI2HD-T2) acceptor. Copolymer P1 is found to be the optimal polymer donor for the fullerene-based solar cells due to its high light absorption, whereas the highest power conversion efficiency of 6.81% is achieved for the all-PSCs with P3, which has the most complementary light absorption with P(NDI2HD-T2).

1. Introduction

Bulk heterojunction (BHJ)-type polymer solar cells (PSCs) have become a promising renewable energy technology that offers great potential for utilization in upcoming commercial devices owing to their lightweight, flexibility, solution processability, and low-cost manufacturing.[1] Among the PSC materials developed to date, fullerene derivatives, such as phenyl-C_{61}-butyric acid methyl ester (PCBM), are the most extensively used electron acceptors. However, PCBM derivatives possess intrinsic disadvantages, including limited energy-level tunability, poor light-absorption ability in the visible and IR range, and poor endurance against thermal, photo, and mechanical stresses.[2] To overcome the issues associated with fullerenes, polymer acceptors have recently emerged to pair with polymer donors to produce all-polymer solar cells (all-PSCs).[3] However, the power conversion efficiency (PCE) of all-PSCs remains inferior to that of fullerene-based PSCs, mainly due to low electron mobility, inefficient charge generation, and unoptimized morphological properties that result in low fill factor (FF) and short-circuit current density (J_{sc}) values. Surprisingly, while all-PSCs advantageously allow independent tuning of the light absorption characteristics of polymer donor and acceptor to maximize harvesting of solar irradiation, this has not yet been fully harnessed to optimize all-PSC performance. It is not trivial to develop polymer donor and acceptor pairs with complementary light absorption as well as desired morphological and electronic properties.[4] Indeed, most of the high-performance all-PSCs reported to date include polymer donor and acceptor components with extensively overlapped light absorption spectra.[3a,c,f,g,5] For example, all-PSCs based on one of the most extensively studied polymer donor and acceptor pairs, poly[4,8-bis(5-(2-ethylhexyl)thiophen-2-yl)benzo[1,2-b:4,5-b']dithiophene-alt-3-fluorothieno[3,4-b]thiophene-2-carboxylate] (P(BDTT-alt-TT-F)), and naphthalene diimide-based polymer acceptors (i.e., N2200 and poly{[N,N'-bis(2-hexyldecyl)-naphthalene-1,4,5,8-bis(dicarboximide)-2,6-diyl]-alt-5,5'-(2,2'-bithiophene)} (P(NDI2HD-T2)), exhibited PCEs

S. W. Kim, J. Choi, C. Lee, J. Jung, Prof. B. J. Kim
Department of Chemical and Biomolecular Engineering
Korea Advanced Institute of Science and Technology (KAIST)
Daejeon 34141, Republic of Korea
E-mail: bumjoonkim@kaist.ac.kr
Dr. T. T. T. Bui, Dr. C. E. Song, Dr. W. S. Shin
Center for Solar Energy Materials
Korea Research Institute of Chemical Technology (KRICT)
Daejeon 34114, Republic of Korea
E-mail: shinws@krict.re.kr
Dr. C. Cho, K. Na, Prof. J.-Y. Lee
Graduate School of Energy Environment Water and Sustainability (EEWS)
Korea Advanced Institute of Science and Technology (KAIST)
Daejeon 34141, Republic of Korea
Prof. B. Ma
Department of Chemical and Biomedical Engineering
Florida State University
Tallahassee, FL 32310, USA

The ORCID identification number(s) for the author(s) of this article can be found under https://doi.org/10.1002/adfm.201703070.

**ADVANCED
SCIENCE NEWS**
www.advancedsciencenews.com

**ADVANCED
FUNCTIONAL
MATERIALS**
www.afm-journal.de

of 5–7%.[3c,6] However, despite extensive optimization of device fabrication conditions, the J_{sc} and PCE values of this system have not increased, likely due to the largely overlapped light absorption of P(BDTT-*alt*-TT-F) and naphthalene-diimide-based polymer acceptors in the wavelength range of 500–800 nm.[3c,6]

Herein, we report the synthesis, properties, and PSC performance of a series of random copolymers with different compositions of the electron-rich unit (D), 2-ethylhexylthienyl substituted benzo[1,2-b:4,5-b']dithiophene (BDTT), and the electron-deficient unit (A), fluorinated thieno[3,4-b]thiophene (TT-F). By controlling the molar ratio between D and A, from 1:1 (P1), to 3:1 (P2), 5:1 (P3), and 7:1 (P4), the optical and electrochemical properties of these polymers were modulated, with the structural and morphological properties largely unchanged.[7] All-PSCs have been fabricated from blends of these D–A random copolymers and P(NDI2HD-T2) acceptors, and a PCE of 6.81% was achieved for devices containing P3:P(NDI2HD-T2) blend active layers, attributed to the complementary absorption properties of the polymer donor and acceptor pairs. This device outperformed all other all-PSCs in this study, including the control P(BDTT-*alt*-TT-F) (P1):P(NDI2HD-T2) device (PCE = 5.74%). The importance of complementary light absorption for highly efficient all-PSCs was also shown by comparing to analogous devices with PCBM acceptors (PCBM-PSCs). Due to the narrow range of light absorption by PCBM,[8] the performance of PCBM-PSCs was limited by light absorption

of polymer donors and the P1 polymer was found to be the optimal polymer donor for the PCBM-PSCs due to the lowest band gap of P1 among the polymer donors.

2. Results and Discussion

A series of P(BDTT-*r*-TT-F) random copolymers with BDTT to TT-F ratios of 3:1 (P2), 5:1 (P3), and 7:1 (P4) was synthesized by Stille coupling in a mixture of toluene and *N,N*-dimethylformamide with Pd(PPh$_3$)$_4$ as the catalyst. The alternating copolymer, P(BDTT-*alt*-TT-F) with 1:1 BDTT:TT-F (P1) was also prepared as a reference due to its excellent performance in PSCs and high compatibility with the P(NDI2HD-T2) acceptor.[9] **Figure 1**a shows the molecular structures of the D–A random copolymers, as well as polymer acceptor P(NDI2HD-T2). In these polymer donors, the BDTT unit provides a planar polymer backbone with low steric hindrance between adjacent branched side chains, while the fluorine-containing TT-F unit was selected due to the ability of fluorine to effectively decreases the highest occupied molecular orbital (HOMO) level.[10] Varying the ratio of D to A units was anticipated to allow fine-tuning of the optical and electrochemical properties.[11] The synthetic routes yielding P1–P4 are shown in Figure S1 in the Supporting Information. The number average molecular weight (M_n) and dispersity (Đ) of the synthesized polymers were measured by size
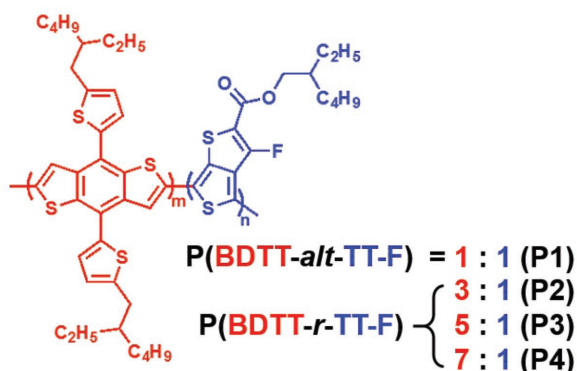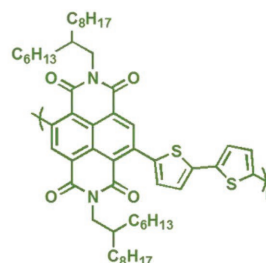
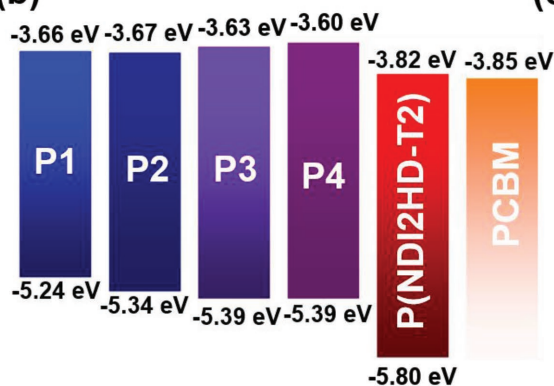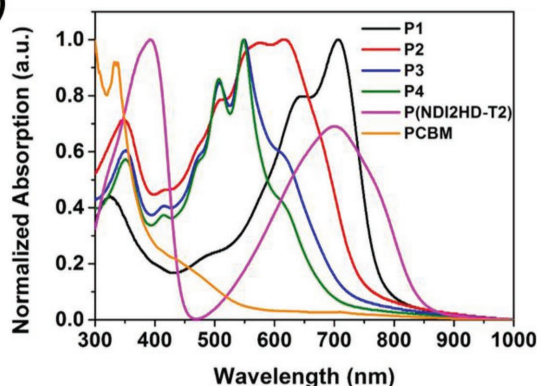**Figure 1.** a) Chemical structures, b) energy level diagram, and c) normalized absorption of P(BDTT-*alt*-TT-F) alternating copolymer (P1), P(BDTT-*r*-TT-F) random copolymers (P2, P3, and P4), and P(NDI2HD-T2) polymer.

**ADVANCED
SCIENCE NEWS**
www.advancedsciencenews.com

**ADVANCED
FUNCTIONAL
MATERIALS**
www.afm-journal.de

Table 1. Characteristics of the polymer donors and acceptors in this study.

Polymer	Feed ratio	Actual ratio[a]	M_n[b] [kg mol^{-1}]	Đ[b] [M_w/M_n]	λ_{max}[c] [nm]	E_g^{opt}[c] [eV]	HOMO [eV]	LUMO [eV]
P1	1:1	1.00:1.00	22.2	2.5	703	1.58	−5.24[d]	−3.66[e]
P2	3:1	3.06:1.00	16.4	2.6	615	1.67	−5.34[d]	−3.67[e]
P3	5:1	5.15:1.00	32.0	3.7	551	1.76	−5.39[d]	−3.63[e]
P4	7:1	7.14:1.00	27.4	3.1	548	1.79	−5.39[d]	−3.60[e]
P(NDI2HD-T2)	–	–	61.0	2.9	392	1.45	−5.80[d]	−3.82[d]

[a]Molar ratio of BDTT and TT-F units, as determined from ^{1}H NMR spectroscopy; [b]Determined by SEC calibrated with polystyrene standards; [c]Determined from the absorption onset in the UV–vis spectra of thin films; [d]Measured by cyclic voltammetry; [e]LUMO = HOMO + E_g^{opt}.

exclusion chromatography (SEC) in *o*-dichlorobenzene at 80 °C. **Table 1** summarizes the composition, molecular weight, and electrochemical properties of the polymer donors. The ratios between BDTT and TT-F in the polymers were determined by ^{1}H NMR spectroscopy (Figure S2, Supporting Information), which show good agreement with the feed ratios used in the polymerizations. The electrochemical properties of P1–P4 polymers were investigated using cyclic voltammetry. The HOMO energy levels of P1–P4 were determined to be −5.24 eV (P1), −5.34 eV (P2), −5.39 eV (P3), and −5.39 eV (P4), showing that the HOMO levels gradually decreased with increasing BDTT content. The lower HOMO levels can lead to higher V_{oc} by producing a larger gap between the lowest unoccupied molecular orbital (LUMO) level of the polymer acceptor.[12] The LUMO levels estimated from LUMO = HOMO + E_g^{opt} (optical band gap) were −3.66 eV (P1), −3.67 eV (P2), −3.63 eV (P3), and −3.60 eV (P4), respectively. Considering the HOMO and LUMO energy levels of P1–P4, all polymers have sufficient driving force to enable efficient exciton dissociation at the donor–acceptor interface.[13]

The optical properties of the polymer donors and polymer acceptor in thin films are shown in Figure 1c. The E_g^{opt} values of films of P1–P4 were estimated to be 1.58, 1.67, 1.76, and 1.79 eV, respectively, based on the onset of light absorption obtained from the UV–vis spectra. Hence, the absorption onset for P1–P4 gradually blueshifted with increasing amounts of the electron-rich BDTT unit.[14] Additionally, the maximum absorption peaks (λ_{max}) values were significantly blueshifted with increasing BDTT composition, from 703 (P1), 615 (P2), 551 (P3), and 548 nm (P4). Thus, it was evident that the colors of the polymer donor pristine films varied from the blue color of the P1 films to purple in P4 films (Figure S3, Supporting Information). P1–P4 polymers showed two main absorption peaks in the visible range, attributed to intramolecular charge transfer and aggregation.[15] The absorption coefficients of the pristine P1–P4 polymer films are given in Figure S3 in the Supporting Information. The maximum absorption coefficients of all of the polymers exceeded 6.7×10^4 cm^{-1}, with values of 8.9×10^4 cm^{-1} for P1, 6.7×10^4 cm^{-1} for P2, 7.2×10^4 cm^{-1} for P3, and 7.2×10^4 cm^{-1} for P4 films. The alternating copolymer P1 had a higher absorption coefficient than the random copolymers P2–P4, due to stronger intermolecular interaction of P1 owing to the regular monomer sequence.[14] In comparison, the P(NDI2HD-T2) absorption spectra contained two absorption bands, at 300–450 and 600–800 nm and yielded the highest

maximum light absorption coefficient of 5.8×10^4 cm^{-1}.[6e,f] Therefore, we anticipated polymer donors that absorb strongly between 450 and 650 nm so as to complement the light absorption of the polymer acceptor in the visible range would exhibit favorable solar cell performance.

To investigate the effect of tuning the light absorption window of the polymer donors on photocurrent generation in all-PSCs, four different polymer donors (P1–P4) were blended with the P(NDI2HD-T2) acceptor to fabricate all-PSCs. **Figure 2**a presents the current density–voltage (*J–V*) characteristics measured under AM 1.5G illumination at 100 mW cm^{-2}. The detailed device fabrication and characterization for all-PSCs are described in the Experimental Section and the photovoltaic parameters are summarized in **Table 2**. The average PCE was found to increase from 5.63% for the P1-based all-PSC to 6.63% for the P3-based all-PSC. The most efficient P3:P(NDI2HD-T2) device exhibited a PCE close to 7% (6.81%), with a V_{oc} of 0.89 V, a J_{sc} of 14.98 mA cm^{-2}, and an FF of 0.51, significantly outperforming the previously reported results from all-PSCs composed of P1 as the polymer donor and P(NDI2HD-T2) as the acceptor.[6e,f] The V_{oc} values increased with BDTT incorporation, from 0.82 for P1-based, 0.87 for P2-based, and to 0.89 for P3-based and P4-based devices, mainly attributed to the decreased HOMO levels with the number of donor units in the polymer backbone. Importantly, the J_{sc} value (14.40 mA cm^{-2}) of P3:P(NDI2HD-T2) device exceeded those of the P1-based, P2-based, and P4-based devices (13.25, 13.40, and 12.96 mA cm^{-2}, respectively). The highest J_{sc} value realized in the P3:P(NDI2HD-T2) device is attributed to complementary light absorption between P3 and P(NDI2HD-T2) that maximized light absorption across the solar spectrum. The J_{sc} value of P4:P(NDI2HD-T2) device was lower than that of P3:P(NDI2HD-T2), due to the lower absorption of P4 particularly in the range between 550 and 750 nm. The external quantum efficiency (EQE) spectra in Figure 2b clearly show how the complementary light absorption of the donor and acceptor components maximizes light absorption in the visible range, as in P3:P(NDI2HD-T2) mixtures, which affects photocurrent generation.

To further demonstrate the importance of complementary light absorption by the polymer acceptor and donor on device performance, we fabricated and characterized PCBM-PSCs with the four polymer donors (P1–P4). While the PCBM-PSC devices exhibit higher efficiency when phenyl-C$_{71}$-butyric acid methyl ester (PC$_{71}$BM) is used,[16] we applied PCBM in order
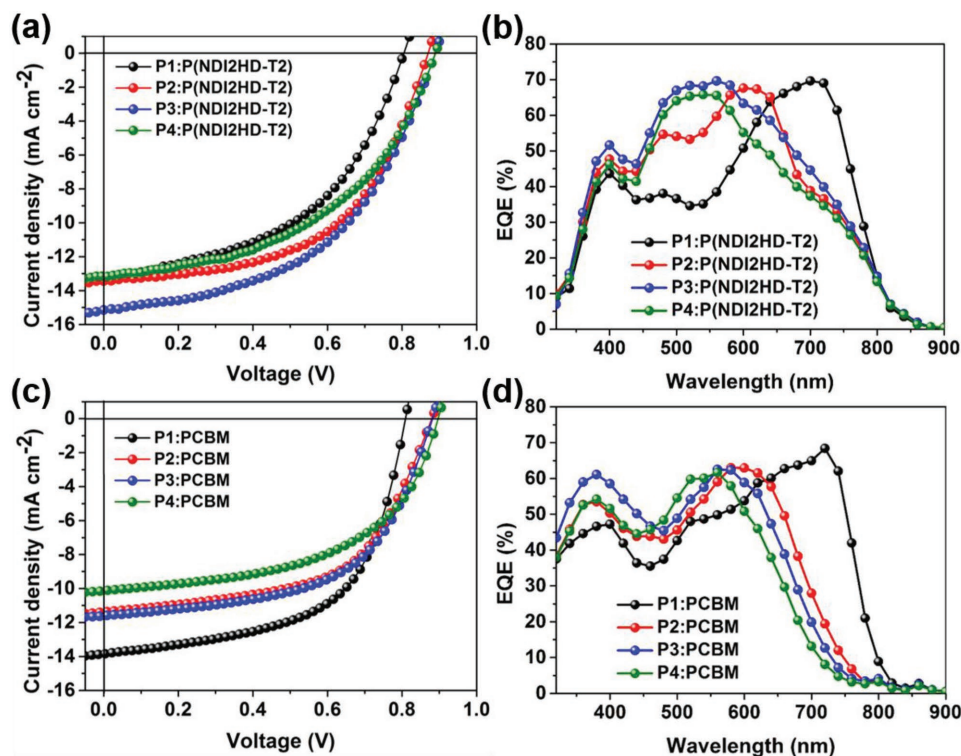
Figure 2. a) Current–voltage (*J–V*) curves and b) external quantum efficiency (EQE) characteristics of the P1–P4:P(NDI2HD-T2) all-PSCs; c) *J–V* curves and d) EQE characteristics of the P1–P4:PCBM-PSCs.

to elucidate the effect of light absorption by the acceptor. In contrast to the trends in all-PSC system, the PCE was significantly decreased when the D:A ratio of the polymer donor was increased, from 6.47% for P1:PCBM to 4.66% for P4:PCBM. These decreased PCEs were mainly attributed to the decreased J_{sc} values from 13.76 for P1:PCBM to 10.06 mA cm^{-2} for P4:PCBM, which were supported by the EQE spectra in Figure 2d. Unlike P(NDI2HD-T2), which exhibits strong light absorption in visible range, PCBM has very weak absorption in the visible region.[16] As a result, the light absorption of polymer-PCBM blends is mainly dictated by that of the polymer donor. Therefore, it is not surprising to see that P1, having lowest band gap and strongest overlap with the solar spectrum, afforded the best device performance. These experiments revealed different

trends in the J_{sc} values of all-PSCs and PCBM-PSCs as a function of polymer donor composition and demonstrated the benefit of employing polymer acceptor components that strongly absorb light in the visible range.

We next investigated the morphological properties of the BHJ blends using grazing-incidence X-ray scattering (GIXS) and atomic force microscopy (AFM), to ensure morphology indeed playing a minimum role in achieving the distinct device performance. In the films, all of the D–A random copolymers showed the preferential "face-on" orientation of the polymer crystalline structures, as evidenced by strong π–π (010) stacking in the out-of-plane direction. Figure S4 and Table S1 in the Supporting Information show similar (d_{100}) lamellar spacing (≈23.1 Å) and π–π stacking spacing (d_{010}) (≈4.1 Å) for P1, P2, P3, and P4 films,

Table 2. Photovoltaic properties of all-PSCs and PCBM-PSCs.

	Active layer	V_{oc} [V]	J_{sc} [mA cm^{-2}]	FF	PCE$_{avg}$[a] (PCE$_{max}$) [%]	Calculated J_{sc} [mA cm^{-2}]	G_{max} [m^{-3} s^{-1}]
All-PSCs	P1:P(NDI2HD-T2)	0.82	13.25	0.52	5.63 (5.74)	13.17	10.18 × 10^{27}
	P2:P(NDI2HD-T2)	0.87	13.40	0.54	6.30 (6.53)	13.32	10.25 × 10^{27}
	P3:P(NDI2HD-T2)	0.89	14.40	0.52	6.63 (6.81)	14.35	11.27 × 10^{27}
	P4:P(NDI2HD-T2)	0.89	12.96	0.48	5.54 (5.69)	12.79	9.73 × 10^{27}
PCBM-PSCs	P1:PCBM	0.81	13.76	0.58	6.47 (6.57)	13.63	8.96 × 10^{27}
	P2:PCBM	0.88	11.43	0.56	5.63 (5.65)	11.32	7.87 × 10^{27}
	P3:PCBM	0.88	11.13	0.57	5.58 (5.75)	10.96	7.30 × 10^{27}
	P4:PCBM	0.89	10.06	0.52	4.66 (4.81)	9.94	6.40 × 10^{27}

[a] The average PCEs were obtained from at least ten different devices for each system.

**ADVANCED
SCIENCE NEWS**
www.advancedsciencenews.com

**ADVANCED
FUNCTIONAL
MATERIALS**
www.afm-journal.de

which agree well with the previously reported values for P1 films.[6h,17] The d_{010} spacing of P1 ($\approx$4.0 Å) was slightly smaller than the other polymers, attributed to the regular D–A sequence in the P1 polymer that produces a tighter packing structure. GIXS of the polymers in the blend films of donor and acceptor polymers showed a similar trend (Figure S5 and Table S2, Supporting Information). The AFM images in Figure S6 in the Supporting Information revealed similar smooth surfaces for all blended films, with low root-mean-square roughness values, ranging from 1.3 to 1.5 nm. The hole and electron mobilities of the P1–P4 neat films and P1–P4:P(NDI2HD-T2) blend films were measured by employing the space charge limited current method (Table S3, Supporting Information).[18] The hole mobilities of the neat polymers (P1–P4) exhibited comparable values on the order of 10^{-4} cm^2 V^{-1} s^{-1}. The all-PSCs fabricated with different polymer donors also showed comparable electron and hole mobilities on the order of 10^{-5} cm^2 V^{-1} s^{-1}. Considering all of the combined morphological and electrical results above, the compositional changes in the polymer donors had marginal influence on the structural and morphological properties of the devices, thus making our system ideal for studying the effects of light absorption of the active layer components on device performance.

To gain deeper insight into the relationship between light absorption and photocurrent generation in the devices, the maximum exciton generation rate (G_{max}) of the devices was calculated by plotting the photocurrent density (J_{ph}) as a function of effective voltage (V_{eff}) (**Figure 3**). G_{max} depends on the maximum number of absorbed photons.[19] Assuming that all of the photogenerated excitons are dissociated to free charges and then collected by the electrode at high electric field, the J_{ph} values became saturated at J_{sat} at a sufficiently high V_{eff}. Thus, G_{max} of the device can be calculated using the equation, $J_{sat} = q \times G_{max} \times L$, where q is the electronic charge and L is the thickness of the active layer in the device.[20] The G_{max} values of all of the devices fabricated with optimized conditions are summarized in Table 2. Among the all-PSCs, the P3:P(NDI2HD-T2) device was calculated to have the highest G_{max} value of 11.27×10^{27} m^{-3} s^{-1}, while the P1:P(NDI2HD-T2), P2:P(NDI2HD-T2), and P4:P(NDI2HD-T2) devices yielded lower G_{max} values of 10.18×10^{27}, 10.25×10^{27}, and 9.73×10^{27} m^{-3} s^{-1}, respectively. For the PCBM-PSCs, the P1-based device exhibited the highest G_{max} value of 8.96×10^{27} m^{-3} s^{-1}. As D:A ratio increased in the

copolymer donors, the G_{max} value decreased gradually to 6.40×10^{27} m^{-3} s^{-1} (P4:PCBM device). Different trends between the G_{max} values of the all-PSCs and PCBM-PSCs with respect to the D:A ratio in the donor polymer are attributed to the difference in light absorption of the polymer and fullerene acceptors for exciton generation.[3l,9b,16b] These findings further suggest that the changes in the J_{sc} values of the devices result mainly from the difference in the number of the absorbed photons in each of the different active layer blends (Figure S7, Supporting Information).

To understand the photocurrent contributions from the donor copolymers (P_D) and acceptors, P(NDI2HD-T2) (P_A) and PCBM, in the active layers, we estimated the compositional EQE contributions of four active layer blends, (P1:P(NDI2HD-T2), P3:P(NDI2HD-T2), P1:PCBM, and P3:PCBM) (**Figure 4**), from the fractional contributions of donor (C_D) and acceptor (C_A) absorbance to the total absorbance of the blend as shown in Figure S9 and Table S4 in the Supporting Information.[6b] It should be noted that a larger contribution from P_D was found in all-PSCs compared to that of the corresponding PCBM-PSC films. The P_D:acceptor blend ratio yielding the highest PCEs in all-PSCs and PCBM-PSCs were 1.5:1 (w/w) and 1:1.5 (w/w), respectively. The partial EQEs of the donor and acceptor components were obtained from the fractional absorbance, assuming similar internal quantum efficiencies among materials. The partial photocurrent contributions of the P_DS and acceptors in the devices were then determined by integrating the partial EQEs multiplied by the AM 1.5G spectrum (**Table 3**). The photocurrent contribution from the P3 donor in the P3:P(NDI2HD-T2) device was estimated to be 10.49 mA cm^{-2}, which is 13% higher than that of the P1 donor in the P1:P(NDI2HD-T2) device (9.29 mA cm^{-2}), despite the lower maximum absorption coefficient of P3 compared to that of P1. This can be explained by the substantially greater absorption of P3 compared to P1 between 450 and 600 nm, where the absorption of P(NDI2HD-T2) is weak, such that the overall absorption spectrum of the P3:P(NDI2HD-T2) blend better matches that of the solar spectrum. In contrast, in PCBM-PSCs, when P1 was replaced by P3, the photocurrent contributions of both P_D and PCBM in the devices decreased. The photocurrent contributions of P_D and PCBM in the P3:PCBM device were calculated to be 8.14 and 2.82 mA cm^{-2}, respectively, corresponding to 17% and 26% decreases, respectively, relative to those in the P1:PCBM device. PCBM absorption mainly
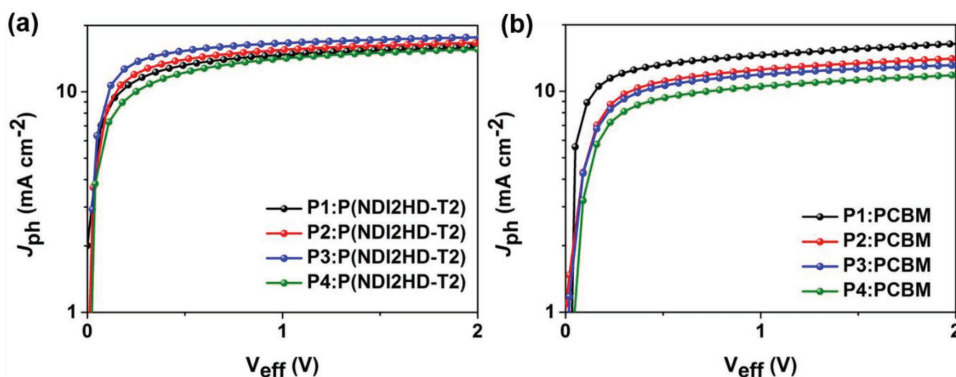

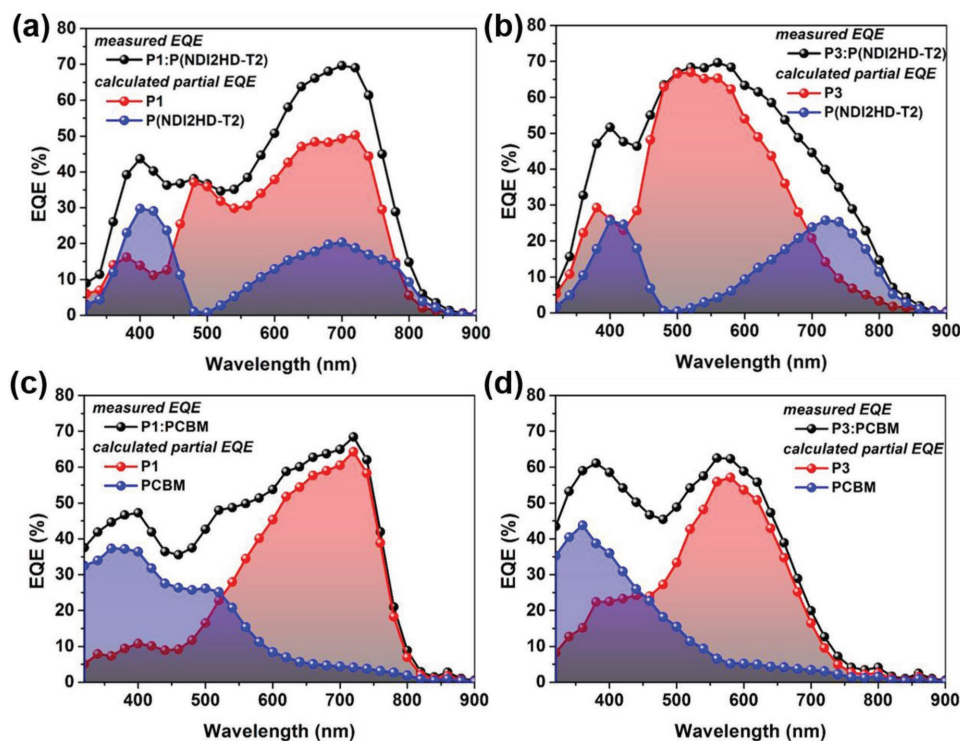**Figure 3.** Photocurrent analysis of a) all-PSCs and b) PCBM-PSCs.

**ADVANCED
SCIENCE NEWS**
www.advancedsciencenews.com

**ADVANCED
FUNCTIONAL
MATERIALS**
www.afm-journal.de

Figure 4. Measured EQEs (black circles) and calculated partial EQEs of donor copolymers (P_D, red circles) and acceptors (P_A or PCBM, blue circles) of devices fabricated with different active-layer blends: a) P1:P(NDI2HD-T2), b) P3:P(NDI2HD-T2), c) P1:PCBM, and d) P3:PCBM.

occurs in the UV range, which increasingly overlaps with the blueshifted donor P3. These results highlight the importance of the design of proper P_D/P_A pairs to exhibit complementary light absorption in order to boost J_{sc} and PCEs in all-PSCs.[21]

3. Conclusion

In summary, we have established synthetic control of light absorption properties for a class of D–A type random copolymers containing different ratios of electron donating BDTT and electron accepting TT-F units and demonstrated the importance of complementary light absorption for producing high-performance all-PSCs. As the D:A ratio was increased from 1:1 to 7:1, the maximum absorption peak of the polymer donors was gradually blueshifted from 703 to 548 nm, which enhanced light absorption of their blends with P(NDI2HD-T2). As a result of improved absorption of the blends over the solar

Table 3. Calculated J_{sc} contributions from absorption of donors and acceptors in P1:P(NDI2HD-T2), P3:P(NDI2HD-T2), P1:PCBM, and P3:PCBM devices.

Active layer	Calculated J_{sc} (P_D) [mA cm^{-2}]	Calculated J_{sc} (P_A or PCBM) [mA cm^{-2}]
P1:P(NDI2HD-T2)	9.29	3.88
P3:P(NDI2HD-T2)	10.49	3.86
P1:PCBM	9.80	3.83
P3:PCBM	8.14	2.82

spectrum, J_{sc} values were significantly enhanced for the all-PSCs, from 13.25 mA cm^{-2} for the P1:P(NDI2HD-T2) device to 14.40 mA cm^{-2} for the P3:P(NDI2HD-T2) device that exhibited a high PCE of 6.81%. In contrast to the all-PSC systems, the PCBM-PSC systems exhibited significantly decreased PCE and J_{sc} values as the D:A ratio of polymer donor increased (P1–P4). Our all-PSCs based on D–A random copolymer donors provided an excellent model system to systematically examine the effect of light absorption of polymers on the device performance without significantly changing the structural and morphological properties. Further, this work emphasizes the advantage of all-PSCs over their polymer-fullerene counterparts, in that the light absorption of both polymer donor and polymer acceptor components can be tuned simultaneously to achieve complementary light absorption to realize higher J_{sc} values, and by extension, overall device efficiencies.

4. Experimental Section

Materials and characterization methods are described in the Supporting Information.

Fabrication of All-PSCs: Inverted type all-PSC devices were fabricated with the structure of indium tin oxide (ITO)/ZnO/active layer (P_D:P(NDI2HD-T2))/MoO$_3$/Ag. The patterned ITO glass was cleaned sequentially with acetone, deionized water, and isopropyl alcohol in an ultrasonic bath for 20 min each. After drying the substrates at 80 °C for 2 h, the ITO substrates were treated in a UV-ozone chamber for 10 min. The fabrication method for each layer is described below. To form the ZnO layer, a ZnO solution was prepared using a sol–gel method, wherein zinc acetate dihydrate (1 g) and ethanolamine (0.28 g) were dissolved in anhydrous 2-methoxy ethanol (10 mL) under vigorous stirring for

more than 24 h. The ZnO thin layer (40 nm) was prepared by spin coating the ZnO solution at 4000 rpm for 40 s, followed by annealing at 200 °C for 15 min in air, and then the devices were moved to a glove box filled with nitrogen gas. Then, a polymer solution in chloroform (CF) (total concentration of 9 mg mL^{-1}) containing P_D:P(NDI2HD-T2) blends with 1,8-diiodooctane (DIO) additive (0.5 vol%) was passed through a 0.2 µm poly(tetrafluoroethylene) (PTFE) filter, spin coated on the ZnO layer to produce the active layer. The blend ratio of P_D:P_A (w/w) and active layer thickness were optimized at 1.5:1 and ≈90 nm, respectively. Finally, the CF and DIO were removed under high vacuum (≈10^{-6} Torr) after 1 h in the glove box. The MoO$_3$ (10 nm) and Ag (120 nm) layers were deposited sequentially onto the active layer via thermal evaporation at about 1×10^{-6} Torr. Using the shadow produced four separated cells on each substrate, devices with an active area of 0.09 cm^2 were produced, as measured by optical microscopy.

Fabrication of PCBM-PSCs: The normal type PCBM-PSC devices were fabricated with the structure of ITO/poly(3,4-ethylenedioxythiophene): poly(styrenesulfonate) (PEDOT:PSS)/active layer (P_D:PC$_{61}$BM)/LiF/Al. ITO substrates were prepared similarly as for all-PSCs. The PEDOT:PSS (PH500) layer (30 nm) was spin coated onto the ITO substrate at 3000 rpm for 40 s and heated at 150 °C for 20 min in air. The devices were then transferred to N$_2$ filled glove box. Polymer solution in chlorobenzene (total concentration of 30 mg mL^{-1}) containing a blend of P_D and PCBM with DIO additive (5 vol%) was passed through a 0.2 µm PTFE filter, spin coated on the PEDOT:PSS layer to produce the active layer. The blend ratio of P_D:PCBM (w/w) and active layer thickness were optimized at 1:1.5 and ≈110 nm, respectively. Finally, thin layers of LiF (0.8 nm) and Al (100 nm) were deposited.

Supporting Information

Supporting Information is available from the Wiley Online Library or from the author.

Conflict of Interest

The authors declare no conflict of interest.

[1] a) C. J. Brabec, S. Gowrisanker, J. J. Halls, D. Laird, S. Jia, S. P. Williams, *Adv. Mater.* **2010**, *22*, 3839; b) C.-C. Chueh, K. Yao, H.-L. Yip, C.-Y. Chang, Y.-X. Xu, K.-S. Chen, C.-Z. Li, P. Liu, F. Huang, Y. Chen, W.-C. Chen, A. K. Y. Jen, *Energy Environ. Sci.* **2013**, *6*, 3241; c) M. Kaltenbrunner, M. S. White, E. D. Glowacki, T. Sekitani, T. Someya, N. S. Sariciftci, S. Bauer, *Nat. Commun.* **2012**, *3*, 770; d) V. Shrotriya, *Nat. Photonics* **2009**, *3*, 447.

[2] a) T. Heumueller, W. R. Mateker, A. Distler, U. F. Fritze, R. Cheacharoen, W. H. Nguyen, M. Biele, M. Salvador, M. von Delius, H.-J. Egelhaaf, M. D. McGehee, C. J. Brabec, *Energy Environ. Sci.* **2016**, *9*, 247; b) S. Savagatrup, A. D. Printz, T. F. O'Connor, A. V. Zaretski, D. Rodriquez, E. J. Sawyer, K. M. Rajan, R. I. Acosta, S. E. Root, D. J. Lipomi, *Energy Environ. Sci.* **2015**, *8*, 55; c) C. B. Nielsen, S. Holliday, H.-Y. Chen, S. J. Cryer, I. McCulloch, *Acc. Chem. Res.* **2015**, *48*, 2803; d) S. M. Ryno, M. K. Ravva, X. Chen, H. Li, J.-L. Brédas, *Adv. Energy Mater.* **2017**, *7*, 1601370; e) M. Jørgensen, K. Norrman, S. A. Gevorgyan, T. Tromholt, B. Andreasen, F. C. Krebs, *Adv. Mater.* **2012**, *24*, 580; f) M. Jørgensen, K. Norrman, F. C. Krebs, *Sol. Energy Mater. Sol. Cells* **2008**, *92*, 686.

[3] a) Y.-J. Hwang, B. A. E. Courtright, A. S. Ferreira, S. H. Tolbert, S. A. Jenekhe, *Adv. Mater.* **2015**, *27*, 4578; b) H. Benten, D. Mori, H. Ohkita, S. Ito, *J. Mater. Chem. A* **2016**, *4*, 5340; c) Z. Li, X. Xu, W. Zhang, X. Meng, W. Ma, A. Yartsev, O. Inganäs, M. R. Andersson, R. A. J. Janssen, E. Wang, *J. Am. Chem. Soc.* **2016**, *138*, 10935; d) Y. Guo, Y. Li, O. Awartani, J. Zhao, H. Han, H. Ade, D. Zhao, H. Yan, *Adv. Mater.* **2016**, *28*, 8483; e) C. Dou, X. Long, Z. Ding, Z. Xie, J. Liu, L. Wang, *Angew. Chem.* **2016**, *55*, 1436; f) J. W. Jung, J. W. Jo, C.-C. Chueh, F. Liu, W. H. Jo, T. P. Russell, A. K.-Y. Jen, *Adv. Mater.* **2015**, *27*, 3310; g) S. Shi, J. Yuan, G. Ding, M. Ford, K. Lu, G. Shi, J. Sun, X. Ling, Y. Li, W. Ma, *Adv. Funct. Mater.* **2016**, *26*, 5669; h) Y. Guo, Y. Li, O. Awartani, H. Han, J. Zhao, H. Ade, H. Yan, D. Zhao, *Adv. Mater.* **2017**, *29*, 1700309; i) B. Fan, L. Ying, Z. Wang, B. He, X.-F. Jiang, F. Huang, Y. Cao, *Energy Environ. Sci.* **2017**, *10*, 1243; j) S. Liu, Z. Kan, S. Thomas, F. Cruciani, J.-L. Bredas, P. M. Beaujuge, *Angew. Chem.* **2016**, *128*, 13190; k) L. Xue, Y. Yang, Z.-G. Zhang, X. Dong, L. Gao, H. Bin, J. Zhang, Y. Yang, Y. Li, *J. Mater. Chem. A* **2016**, *4*, 5810; l) H. Kang, W. Lee, J. Oh, T. Kim, C. Lee, B. J. Kim, *Acc. Chem. Res.* **2016**, *49*, 2424; m) T. Kim, J.-H. Kim, T. E. Kang, C. Lee, H. Kang, M. Shin, C. Wang, B. Ma, U. Jeong, T.-S. Kim, B. J. Kim, *Nat. Commun.* **2015**, *6*, 8547; n) R. Zhao, C. Dou, Z. Xie, J. Liu, L. Wang, *Angew. Chem. Int. Ed.* **2016**, *55*, 5313.

[4] a) L. Gao, Z.-G. Zhang, L. Xue, J. Min, J. Zhang, Z. Wei, Y. Li, *Adv. Mater.* **2016**, *28*, 1884; b) H. Benten, T. Nishida, D. Mori, H. Xu, H. Ohkita, S. Ito, *Energy Environ. Sci.* **2016**, *9*, 135.

[5] a) T. Earmme, Y.-J. Hwang, S. Subramaniyan, S. A. Jenekhe, *Adv. Mater.* **2014**, *26*, 6080; b) Y.-J. Hwang, T. Earmme, S. Subramaniyan, S. A. Jenekhe, *Chem. Commun.* **2014**, *50*, 10801; c) J. Oh, K. Kranthiraja, C. Lee, K. Gunasekar, S. Kim, B. Ma, B. J. Kim, S. H. Jin, *Adv. Mater.* **2016**, *28*, 10016; d) H. Kang, M. A. Uddin, C. Lee, K.-H. Kim, T. L. Nguyen, W. Lee, Y. Li, C. Wang, H. Y. Woo, B. J. Kim, *J. Am. Chem. Soc.* **2015**, *137*, 2359.

[6] a) D. Mori, H. Benten, I. Okada, H. Ohkita, S. Ito, *Energy Environ. Sci.* **2014**, *7*, 2939; b) Z. Li, W. Zhang, X. Xu, Z. Genene, D. Di Carlo Rasi, W. Mammo, A. Yartsev, M. R. Andersson, R. A. J. Janssen, E. Wang, *Adv. Energy Mater.* **2017**, *7*, 1602722; c) X. Long, Z. Ding, C. Dou, J. Zhang, J. Liu, L. Wang, *Adv. Mater.* **2016**, *28*, 6504; d) X. Li, P. Sun, Y. Wang, H. Shan, J. Xu, C. Song, Z.-x. Xu, Z.-K. Chen, *J. Mater. Chem. C* **2016**, *4*, 2106; e) J. Jung, W. Lee, C. Lee, H. Ahn, B. J. Kim, *Adv. Energy Mater.* **2016**, *6*, 1600504; f) W. Lee, C. Lee, H. Yu, D.-J. Kim, C. Wang, H. Y. Woo, J. H. Oh, B. J. Kim, *Adv. Funct. Mater.* **2016**, *26*, 1543; g) P. Deng, C. H. Y. Ho, Y. Lu, H.-W. Li, S.-W. Tsang, S. K. So, B. S. Ong, *Chem. Commun.* **2017**, *53*, 3249; h) H. Kang, K.-H. Kim, J. Choi, C. Lee, B. J. Kim, *ACS Macro Lett.* **2014**, *3*, 1009.

**ADVANCED
SCIENCE NEWS**

www.advancedsciencenews.com

**ADVANCED
FUNCTIONAL
MATERIALS**

www.afm-journal.de

[7] T. T. T. Bui, M. Jahandar, C. E. Song, Q. V. Hoang, J.-C. Lee, S. K. Lee, I.-N. Kang, S.-J. Moon, W. S. Shin, *Sol. Energy Mater. Sol. Cells* **2015**, *134*, 148.

[8] a) Y. Lin, Y. Li, X. Zhan, *Chem. Soc. Rev.* **2012**, *41*, 4245; b) J. T. Bloking, T. Giovenzana, A. T. Higgs, A. J. Ponec, E. T. Hoke, K. Vandewal, S. Ko, Z. Bao, A. Sellinger, M. D. McGehee, *Adv. Energy Mater.* **2014**, *4*, 1301426; c) Y.-J. Cheng, S.-H. Yang, C.-S. Hsu, *Chem. Rev.* **2009**, *109*, 5868; d) G. Zhao, Y. He, Y. Li, *Adv. Mater.* **2010**, *22*, 4355.

[9] a) L. Lu, W. Chen, T. Xu, L. Yu, *Nat. Commun.* **2015**, *6*, 7327; b) Y. Lin, J. Wang, Z.-G. Zhang, H. Bai, Y. Li, D. Zhu, X. Zhan, *Adv. Mater.* **2015**, *27*, 1170; c) S.-H. Liao, H.-J. Jhuo, Y.-S. Cheng, S.-A. Chen, *Adv. Mater.* **2013**, *25*, 4766.

[10] a) H.-Y. Chen, J. Hou, S. Zhang, Y. Liang, G. Yang, Y. Yang, L. Yu, Y. Wu, G. Li, *Nat. Photonics* **2009**, *3*, 649; b) J. Hou, H.-Y. Chen, S. Zhang, R. I. Chen, Y. Yang, Y. Wu, G. Li, *J. Am. Chem. Soc.* **2009**, *131*, 15586; c) L. Lu, L. Yu, *Adv. Mater.* **2014**, *26*, 4413.

[11] a) S. Noh, N. S. Gobalasingham, B. C. Thompson, *Macromolecules* **2016**, *49*, 6835; b) N. S. Gobalasingham, S. Noh, J. B. Howard, B. C. Thompson, *ACS Appl. Mater. Interfaces* **2016**, *8*, 27931; c) T. E. Kang, K.-H. Kim, B. J. Kim, *J. Mater. Chem. A* **2014**, *2*, 15252; d) X. Li, P. Sun, Y. Wang, H. Shan, J. Xu, C. You, Z.-x. Xu, Z.-K. Chen, *Polym. Chem.* **2016**, *7*, 2230; e) T. E. Kang, H.-H. Cho, H. J. Kim, W. Lee, H. Kang, B. J. Kim, *Macromolecules* **2013**, *46*, 6806.

[12] a) M. Lenes, S. W. Shelton, A. B. Sieval, D. F. Kronholm, J. C. Hummelen, P. W. M. Blom, *Adv. Funct. Mater.* **2009**, *19*, 3002; b) H. Kang, C.-H. Cho, H.-H. Cho, T. E. Kang, H. J. Kim, K.-H. Kim, S. C. Yoon, B. J. Kim, *ACS Appl. Mater. Interfaces* **2012**, *4*, 110.

[13] a) D. Veldman, S. C. J. Meskers, R. A. J. Janssen, *Adv. Funct. Mater.* **2009**, *19*, 1939; b) T. E. Kang, H.-H. Cho, C.-H. Cho, K.-H. Kim, H. Kang, M. Lee, S. Lee, B. S. Kim, C. Im, B. J. Kim, *ACS Appl. Mater. Interfaces* **2013**, *5*, 861.

[14] T. E. Kang, J. Choi, H.-H. Cho, S. C. Yoon, B. J. Kim, *Macromolecules* **2016**, *49*, 2096.

[15] H. Zhong, C.-Z. Li, J. Carpenter, H. Ade, A. K.-Y. Jen, *J. Am. Chem. Soc.* **2015**, *137*, 7616.

[16] a) F. Zhang, Z. Zhuo, J. Zhang, X. Wang, X. Xu, Z. Wang, Y. Xin, J. Wang, J. Wang, W. Tang, Z. Xu, Y. Wang, *Sol. Energy Mater. Sol. Cells* **2012**, *97*, 71; b) Y. He, Y. Li, *Phys. Chem. Chem. Phys.* **2011**, *13*, 1970.

[17] a) B. Wang, W. Liu, H. Li, J. Mai, S. Liu, X. Lu, H. Li, M. Shi, C.-Z. Li, H. Chen, *J. Mater. Chem. A* **2017**, *5*, 9396; b) M. Li, Y. Liu, W. Ni, F. Liu, H. Feng, Y. Zhang, T. Liu, H. Zhang, X. Wan, B. Kan, Q. Zhang, T. P. Russell, Y. Chen, *J. Mater. Chem. A* **2016**, *4*, 10409.

[18] D. Chirvase, Z. Chiguvare, M. Knipper, J. Parisi, V. Dyakonov, J. C. Hummelen, *J. Appl. Phys.* **2003**, *93*, 3376.

[19] J.-L. Wu, F.-C. Chen, Y.-S. Hsiao, F.-C. Chien, P. Chen, C.-H. Kuo, M. H. Huang, C.-S. Hsu, *ACS Nano* **2011**, *5*, 959.

[20] a) V. D. Mihailetchi, H. Xie, B. de Boer, L. J. A. Koster, P. W. M. Blom, *Adv. Funct. Mater.* **2006**, *16*, 699; b) K.-H. Kim, H. Kang, H. J. Kim, P. S. Kim, S. C. Yoon, B. J. Kim, *Chem. Mater.* **2012**, *24*, 2373.

[21] a) S. Li, L. Ye, W. Zhao, S. Zhang, S. Mukherjee, H. Ade, J. Hou, *Adv. Mater.* **2016**, *28*, 9423; b) S. Chen, Y. Liu, L. Zhang, P. C. Y. Chow, Z. Wang, G. Zhang, W. Ma, H. Yan, *J. Am. Chem. Soc.* **2017**, *139*, 6298.

1703070 (8 of 8)